Chain Packing in Linear Phenol−Polycarbonate by $^{13}C\{^2H\}$ REDOR

Robert D. O'Connor,[†] Barbara Poliks,[‡] Daniel H. Bolton,[†,§] Jon M. Goetz,[†,#] Jeffery A. Byers,[†] Karen L. Wooley,[†] and Jacob Schaefer*[,†]

Department of Chemistry, Washington University, St. Louis, Missouri 63130, and Department of Physics, Binghamton University, Binghamton, New York 13902

Received May 29, 2001

ABSTRACT: Interchain packing in [carbonyl-^{13}C, phenol-^2H]phenol-substituted bisphenol A polycarbonate (a totally amorphous polymer by X-ray powder diffraction) has been characterized by $^{13}C\{^2H\}$ rotational-echo double-resonance (REDOR) NMR measurements on a 10 Å distance scale. Differences in the REDOR dephasing rates of the centerband and spinning sidebands of the carbonyl carbon resonance prove the presence of local orientational order. Approximately 70% of the repeat units are locally ordered. For the most tightly packed pairs of chains, the phenol ^2H of one chain is 4−5 Å from the carbonate ^{13}C of the other chain, and the interchain $^2H-^{13}C$ dipolar vector has an orientation of approximately 30° (azimuthal) and 70° (polar) in the carbonyl carbon chemical shift tensor reference frame. The REDOR determination of these packing parameters is model-independent. Both random and chain-pair models were generated to describe the chain packing, but only the chain-pair model was consistent with the REDOR distance and orientation results.

Introduction

Currently there are two approaches to the description of chain packing in polycarbonate: one starts from the notion that the chain packing is homogeneous, or random, like that in a nearly isotropic melt or rubber, but with some local ordering superimposed;[1−3] the other description starts from the notion that the chain packing in polycarbonate is more crystalline-like, but with very small ordered domains, consisting of only a few repeat units of a few proximate chains.[4,5] These domains are themselves imperfect, vary in size from 10 Å to no more than 50 Å, and are randomly packed with respect to one another in a globally disorganized matrix. Both descriptions are in agreement with the fact (established by diffraction experiments) that there is no long-range order in a polycarbonate glass.[6,7]

In this paper we describe the use of $^{13}C\{^2H\}$ rotational-echo double resonance[8] (REDOR) to characterize the extent of local order in the chain packing of a $^{13}C,^2H$-labeled phenol-substituted bisphenol A polycarbonate. This polycarbonate has one isopropylidene methyl group replaced by a phenol ring. All of the carbonate carbonyl carbons are ^{13}C labeled, and approximately 65% of the hydroxyl protons are replaced by ^2H labels. The observed $^{13}C\{^2H\}$ REDOR dephasing provides direct structural information on the packing of nearest-neighbor chains and leads to the conclusion that about 70% of the chains in the glass are locally ordered with respect to their nearest neighbors.

Experimental Methods

Synthesis. Synthesis of the phenol-substituted bisphenol A polycarbonate was achieved in three steps as appears in Scheme 1. The formation and isolation of the monobenzylated product from 1,1,1-tris(4′-hydroxyphenyl)ethane gave a diphe-

Scheme 1

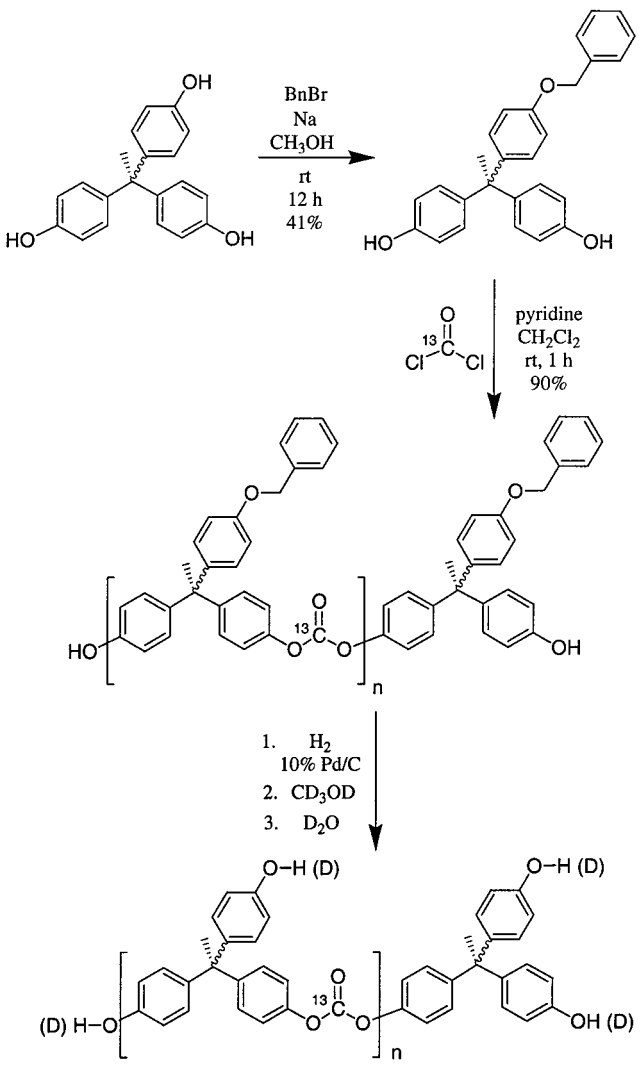

[†] Washington University.
[‡] Binghamton University.
[§] Present address: Bayer Plastics Division, Pittsburgh, PA 15205.
[#] Present address: Varian Associates, Palo Alto, CA 94304.
* Corresponding author: phone 314-935-6844; Fax 314-935-4481; e-mail schaefer@wuchem.wustl.edu.

10.1021/ma010919i CCC: $22.00
Published on Web 02/28/2002

nolic A−A monomer that was necessary for linear polycarbonate growth. Polymerization of the benzyl-protected monomer was achieved by condensation with ^{13}C-labeled phosgene (Isotec, 99% ^{13}C, as a 1.1 M solution in benzene). Deprotection of the benzyl group was then performed by hydrogenolysis to give a phenol-substituted bisphenol A polycarbonate. Deuterium exchange by precipitation into deuterated methanol then afforded the [carbonyl-^{13}C, phenol-^{2}H]phenol-substituted bisphenol A polycarbonate.

1,1-Bis(4′-hydroxyphenyl)-1-(4′-benzyloxyphenyl)ethane. Under nitrogen, sodium (0.765 g, 33.3 mmol) was added to methanol (500 mL) and allowed to stir for 0.5 h; 1,1,1-tris-(4′-hydroxyphenyl)ethane (10.89 g, 35.55 mmol) was added to the sodium methoxide solution and allowed to equilibrate for 0.5 h. Benzyl bromide (5.662 g, 33.10 mmol) dissolved in methanol (200 mL) was added dropwise to the phenoxide solution. The reaction was allowed to stir at room temperature overnight. The methanol was removed under reduced pressure. Most of the organic material was dissolved upon addition of diethyl ether (50 mL) to the resulting pink residue. Dissolution of the insoluble material occurred when the organic layer was extracted with 5% $HCl_{(aq)}$. The organic layer was subsequently washed with 5% $NaHCO_{3(aq)}$, washed with water, and dried over $MgSO_4$. The ether was removed under reduced pressure, and the resulting residue was dissolved in a small amount of CH_2Cl_2 and then purified by flash column chromatography (silica gel, using a gradient solvent system as eluent: CH_2Cl_2 until tri- and dibenzyl-substituted byproduct eluted followed by ether:CH_2Cl_2, 10:90 until the desired monobenzyl-substituted product eluted). The organic solvents were removed in vacuo to give a pale yellow foam. This was recrystallized from CH_2Cl_2 to yield 5.384 g (41%) of the diphenolic monomer as a colorless solid.

General Synthesis of [Carbonyl-^{13}C]phenylbenzyloxy-Substituted Bisphenol A Polycarbonate. Under nitrogen, a 0.15 M solution of 1,1-bis(4′-hydroxyphenyl)-1-(4′-benzyloxyphenyl)ethane was prepared in degassed CH_2Cl_2. Three equivalents of pyridine were added to the solution and allowed to stir for 0.5 h. A stoichiometric amount of ^{13}C-labeled phosgene was then added to the solution and allowed to stir for 0.5 h. Subsequent additions of ^{13}C-labeled phosgene were made at 30 min intervals, while polymer growth was monitored by GPC (based upon calibration with polystyrene standards). Once the polymer had reached the desired molecular weight, CH_2Cl_2 was added, and the reaction mixture was then extracted with 10% $HCl_{(aq)}$ solution followed by 5% aqueous sodium bicarbonate solution. The organic layer was isolated, dried over $MgSO_4$, and concentrated in vacuo. The resulting viscous liquid was dissolved in THF and precipitated into methanol, yielding the polymer as a white powder.

General Synthesis of [Carbonyl-^{13}C, phenol-^{2}H]phenol-Substituted Bisphenol A Polycarbonate. Under nitrogen, a 0.022 M solution of [carbonyl-^{13}C]phenylbenzyloxy-substituted bisphenol A polycarbonate was prepared in dry degassed tetrahydrofuran. A catalytic amount of 10% palladium on carbon was added. The flask was evacuated, and hydrogen gas was introduced at pressures slightly greater than atmospheric. The progress of the hydrogenolysis reaction was followed with ^{1}H NMR (300 MHz using THF-d_8 as the solvent) by comparing the integral value for the benzyl ether methylene protons (appearing at 5.0 ppm) to the integral value of the backbone methyl protons (appearing at 2.1 ppm). When the benzyl ether methylene proton signal had become unobservable, the reaction was stopped by removing the hydrogen atmosphere and filtering off the palladium carbon catalyst. The solution was concentrated, and the product was precipitated into methanol to yield a white to pale yellow solid. Exchange of a portion of the phenolic protons with deuterons to afford the doubly labeled polycarbonate material was then accomplished by dissolution of the [carbonyl-^{13}C]phenol-substituted bisphenol A polycarbonate into tetrahydrofuran, followed by reprecipitation into d_4-methanol. This was followed by a second exchange, dissolving the polymer in tetrahydrofuran and precipitating into excess D_2O, followed by lyophilization at −50 °C. M_w = 30 600 and M_n = 18 400 from GPC based upon calibration with polystyrene standards. T_g = 210 °C. FT-IR: 3600−3200, 3062, 3041, 2978, 2877, 1776, 1612, 1592, 1503, 1440, 1377, 1366, 1235, 1196, 1165, 1115, 1057, 1014, 891, 832 cm^{-1}. ^{1}H NMR (THF-d_8): δ 2.14 (s, 3H, ArCC***H***$_3$), 6.65 and 6.89 (ABq, 4H, ***J*** = 9 Hz, Ar***H***OH), 7.09−7.22 (m, 8H, Ar***H***OCO), 8.19 (s, 1H, ArO***H***) ppm. ^{13}C NMR (THF-d_8): δ 31.18, 52.16, 115.45, 120.93, 130.33, 130.55, 139.88, 148.38, 150.41, 152.48, 156.97 ppm.

REDOR NMR. The ^{13}C NMR spectra were acquired from a 134 mg sample at ambient temperature using a Chemagnetics CMX-300 spectrometer, operating at 75.453 MHz for carbon, and equipped with a three-frequency transmission-line probe.[9] Magic-angle spinning was at 1667 Hz, corresponding to a 600 μs rotor period (T_R). Other experimental conditions included a 2 ms, 50 kHz matched ^{1}H−^{13}C cross-polarization contact, 75 and 80 kHz B_1 fields for the ^{13}C and ^{2}H π pulses, respectively, and 60 kHz proton decoupling. Increasing the decoupling field to 100 kHz did not change the observed line shapes.

REDOR experiments are always done in two parts, once with dephasing pulses and once without.[8] Both parts have the identical number of refocusing pulses. The differences in ^{13}C signal intensities in the two parts of REDOR experiments performed on ^{13}C- and ^{2}H-labeled phenol−polycarbonate (with ^{13}C refocusing pulses and with and without ^{2}H dephasing pulses) are directly related to the corresponding distances between ^{13}C labels and ^{2}H labels. The REDOR pulse sequences that were used had a fixed total of 4, 8, or 16 ^{13}C π pulses, depending on whether the number of rotor cycles in the dipolar evolution could be evenly divided by 4, 8, or 16, respectively.[9] The sequence with eight ^{13}C pulses is illustrated in Figure 1 of ref 9. For 4 and 12 rotor cycles, only 4 ^{13}C π pulses were used; for 8 and 24 rotor cycles, both 4 and 8 ^{13}C π pulses were used in separate experiments; and for 16 and 32 rotor cycles, 4, 8, and 16 ^{13}C π pulses were used in three separate experiments. The phase cycling for the ^{13}C pulses was XY*n*, where *n* equals the number of ^{13}C pulses.[10] The ^{2}H π pulses were XY4 phase cycled.[10] Generally, slightly greater dephasing (1−2%) was observed using more ^{13}C pulses (and, consequently, fewer ^{2}H pulses), presumably because the ^{2}H B_1 field was not large compared to the quadrupolar coupling. All ^{2}H and ^{13}C homonuclear interactions were weak, and their effects were removed by magic-angle spinning.

^{2}H NMR. Quadrupolar-echo ^{2}H NMR spectra were obtained[11] at 61.3 MHz with a 30 μs echo delay, a 2.4 μs π/2 pulse (B_1 = 104 kHz), and a recovery delay of 4 s. All spectra were approximately 90% fully relaxed.

X-ray Diffraction. Powder diffraction patterns of linear phenol−polycarbonate and a noncrystalline hyperbranched polycarbonate[12] were obtained with a Rigaku vertical-power diffractometer equipped with Materials Data Inc. automation and analysis software. The sample mounts were scanned using copper radiation (35 kV and 35 mA) from 5° to 65° (2θ) using a 0.04° step increment and a 1 s dwell time per step.

Molecular Modeling. A structure containing 48 four-unit phenol−polycarbonate chains was built and minimized with the Cerius 2 software of Molecular Simulations Inc., San Diego, using PCFF and COMPASS force fields. Each all-trans chain was generated from an equimolar random mix of the two stereoisomers of the phenol−polycarbonate monomer. The minor population of cis defects likely to be present in phenol−polycarbonate[9] was not included. The resulting 48 chains were mixed by the Cerius 2 software to produce an amorphous polymer having a density of approximately 1.1 g/cm^3. This structure underwent 10 cycles of a simulated annealing process for a total of 4 ps. The starting and mid-cycle temperatures of the annealing were 300 and 500 K, respectively. The temperature was changed in 50 deg increments. Each increment contained 50 1 fs steps of molecular dynamics. The structure was energy-minimized after each cycle. It is referred to in the text as the random-packing model.

A second, partially randomized structure was built that contained 24 pairs of the four-unit phenol−polycarbonate chains. The energy-minimized chains were paired by hand in such a way that the distances between deuterons from one

chain and carbonyl carbons from the second chain were in the range 3−5 Å. This arrangement for polycarbonate chains is known as a Whitney−Yaris pair.[5] Paired chains with varying mainchain direction were then assembled by hand into a cube-shaped structure having a density of about 1 g/cm^3. End effects for the final structure were reduced by melding cubes together. The hand-built cube was energy-minimized in vacuo and underwent the same annealing process as that used for the amorphous polymer. About 120 of the 196 interchain D−C(=O) distances within a cube were still less than 5 Å after the annealing. For these pairs, a second annealing of 30 cycles was run with the O−C(=O)−D angle and D−O−C(=O)−O dihedral angle constrained to reproduce the orientation found experimentally (see below). These constraints did not increase the energy of the system appreciably. This structure is referred to in the text as the chain-pair packing model.

Calculated REDOR Dephasing. On the basis of a 1667 Hz, eight-rotor cycle S_0 spectrum (not shown), the carbonyl carbon chemical shift anisotropy (δ) and asymmetry (η) parameters were estimated to be 86 ppm and 0.44, respectively. These values were needed for the sideband dephasing calculation and are similar to other published results for polycarbonate carbonyl carbons.[2,3] A general expression for the intensity, I_N, of a REDOR dephased sideband is[13]

$$I_N = \int R_D[\Omega; \alpha_D, \beta_D, \lambda_D]\, G_N[\Omega; \delta_{CS}, \eta_{CS}]\, d\Omega \qquad (1)$$

where $G_N[\Omega]$ is the distribution of powder orientations contained in sideband N generated by magic-angle sample spinning at ω_R, and $R_D[\Omega]$ is the orientational dependent REDOR dephasing of a single crystal. The powder angles of each CSA tensor in the rotor frame are given by Ω, the shift-tensor anisotropy and asymmetry by δ and η, respectively, and the orientation of the dipolar tensor relative to the shift tensor by α_D (azimuthal) and β_D (polar) angles; λ_D is the REDOR evolution parameter, which equals the product of the evolution time and dipolar coupling.

The dephasing for the random and chain-pair packing models was calculated as the average over all the carbonyl carbons and included the multispin dephasing of the closest three deuterons. Including more distant deuterons had no substantive effect. The dephasing function $R_D[\Omega]$ in this situation is[13]

$$R_D[\Omega] = \prod_{i=1}^{3} 1 - p_1 - p_2 + p_1 \cos[\Theta_D[\Omega, \alpha_{D,i}, \beta_{D,i}, \lambda_{D,i}]] + p_2 \cos[2\Theta_D[\Omega, \alpha_{D,i}, \beta_{D,i}, \lambda_{D,i}]] \qquad (2)$$

where Θ_D is the phase accumulated from dipolar evolution; $\alpha_{D,i}$ and $\beta_{D,i}$ are the azimuthal and polar angles, respectively, describing the orientation of the ith $^{13}C-^2H$ dipolar tensor (i = 1, 2, 3) in the respective carbonyl carbon CSA reference frame; and $\lambda_{D,i}$ is the corresponding REDOR evolution parameter. The powder average over this multispin $R_D[\Omega]$, multiplied by the appropriate CSA weighting function,[13] yields I_N, the integrated intensity of the Nth spinning sideband after REDOR dephasing.

The parameters p_1 and p_2 were incorporated to compensate for imperfect ^2H pulses. These parameters qualitatively mimic average Hamiltonian parameters describing finite pulses.[14] For perfect ^2H pulses, $p_1 = 0$ and $p_2 = {}^2/_3$. From experiments performed on L-[3-^{13}C, 2-^{2}H]alanine, p_1 and p_2 for our spectrometer were found to be 0.03 and 0.539, respectively.[13] These values suggest that the pulses were about 80% efficient for alanine. Less efficiency can be expected for the phenol−polycarbonate because of the larger quadrupolar coupling (see Figure 1). In all the phenol−polycarbonate calculations, both parameters were set to 0.15. These values were based on calculated matches to the observed quaternary carbon dephasing for long evolution times (see below).

Experimental and calculated values of sideband dephasing were compared using the ratio of the sideband dephasing *relative* to the total dephasing. Comparing ratios is less sensitive to finite-pulse effects than comparing the intensities directly. This ratio is defined as

$$S_N^R = \frac{\Delta I_N \sum_k I_{k,0}}{I_{N,0} \sum_k \Delta I_k} \qquad (3)$$

where the sum over the sideband order (k) ranged from −3, ..., 0, ..., +3 and $\Delta I_k = I_{k,0} - I_k$, with I_k and $I_{k,0}$ equal to the experimental or calculated sideband intensity, with and without dephasing pulses, respectively.

The dephasing for short dipolar evolution times is dominated by the single, nearest-neighbor deuteron. If we assume that only a fraction, f, of the $^{13}C-^2H$ dipolar vectors have the same orientation relative to the carbonyl carbon shift tensor, and the remainder, $1 - f$, are isotropically oriented, then

$$I_N^{observe} = (1 - f) I_N^{isotropic} + f I_N \qquad (4)$$

To obtain f and the orientation of the $^{13}C-^2H$ dipolar tensor of the nearest-neighbor deuteron with respect to the carbonyl carbon chemical shift tensor, an error function, χ^2, was calculated in two-degree angular increments for each orientation ($0 < \alpha_D, \beta_D < 90$):[13]

$$\chi^2[\alpha_D, \beta_D, f] = \sqrt{\sum_{j=1}^{n} \sum_{k=-3}^{3} \left(1 - \frac{1 - f(1 - S_k^R[\alpha_D, \beta_D, \lambda_{D,j}]_{calc(j)})}{S_{k,exp(j)}^R} \right)^2} \qquad (5)$$

where f is the fraction of oriented sample; subscripts exp and calc denote experimental and calculated values, respectively; and j designates various experiments (out of a set of n) with different evolution times and the corresponding λ_D's for the calculated dephasing.

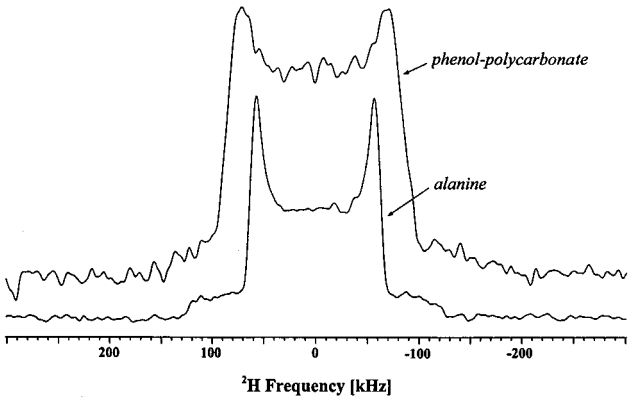

Figure 1. 61.3 MHz quadrupolar-echo ^2H NMR spectra of phenol−polycarbonate with about 65% of the phenol hydroxyls ^2H labeled (top) and crystalline L-[2-^{2}H]alanine (bottom).

Results

^{2}H NMR. The ^2H quadrupolar-echo spectrum of the phenol−polycarbonate shows a broad Pake doublet, consistent with the quadrupolar coupling for an oxygenated deuterium in an asymmetric environment[15] (Figure 1, top). The deuterons appear to be static. There is no evidence in the spectrum for the presence of averaging by fast, large-amplitude motion. Motion in an intermediate-frequency regime is unlikely because no significant line-shape changes were observed when the echo delay time was increased to 300 μs. Finally, two-dimensional ^2H NMR exchange experiments[16] showed no evidence of motion on a millisecond time scale. Spin counts

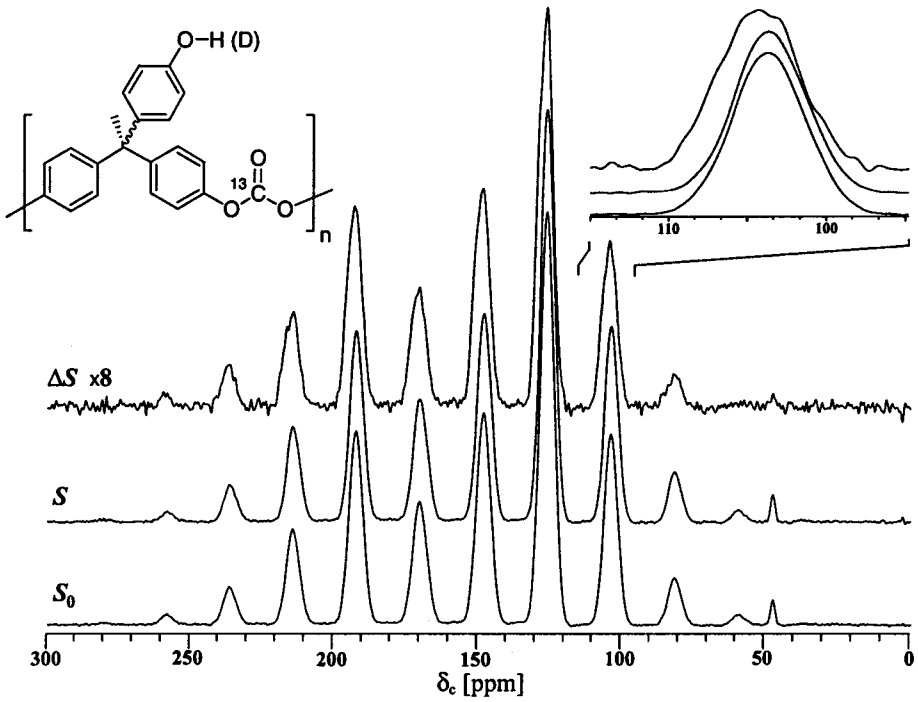

Figure 2. 75 MHz $^{13}C\{^2H\}$ REDOR spectra of linear phenol−polycarbonate after 20 ms of dipolar evolution. All carbonate carbons are ^{13}C-labeled, and about 65% of the phenol hydroxyls are ^2H-labeled. The REDOR difference is shown at the top of the figure, the full echo at the bottom, and the dephased echo in the middle. The centers of the difference peaks are shifted about 1 ppm to low field, relative to those of the dephased echo peaks (inset, right). Each spectrum was the result of the accumulation of 4096 scans. Magic-angle spinning was at 1667 Hz.

calibrated by the ^2H quadrupolar-echo spectrum of L-[2-^2H]alanine (Figure 1, bottom) indicate that about 65 ±5% of the phenols were deuterated.

REDOR Dephasing. The $^{13}C\{^2H\}$ REDOR spectra of the double-labeled phenol−polycarbonate are dominated by the signals arising from the ^{13}C-labeled carbonyl carbon (Figure 2). The centerband resonance appears near 150 ppm; all the other major peaks are spinning sidebands. The only other feature of the spectra that is readily assignable is the quaternary carbon resonance at 47 ppm. The natural abundance, protonated aromatic carbon resonances are expected at 138 ppm,[17] resolved from the carbonyl carbon centerband and sidebands. These peaks have a much shorter T_2 than that of the carbonyl carbon peak and are not visible in Figure 2. The nonprotonated aromatic carbon resonances have shifts that are similar to that of the carbonyl carbon peak but account for less than 5% of the carbonyl carbon peak intensity.[9]

The REDOR difference peaks ($\Delta S = S_0 - S$, where S and S_0 are echo intensities with and without dephasing ^2H pulses, respectively) for the carbonyl carbon are shifted about 1 ppm to low field relative to the shift positions for the full-echo peaks. Thus, the difference spectrum (ΔS) is shifted to the left, and the dephased spectrum (S) to the right, of the full-echo (S_0) spectrum (Figure 2, inset, top right). A similar shift has been observed for the carbonyl carbon ΔS of an ethoxyphenyl-substituted bisphenol A polycarbonate and interpreted in terms of the preference of the carbonate moiety for an extended trans conformation.[9] For phenol−polycarbonate, hydrogen bonding is also a possible contributor to the downfield shift.[18]

The experimental dephasing as a function of the evolution time for the labeled carbonyl carbon and natural abundance quaternary carbon is shown in Figure 3 (symbols). The average standard deviation per

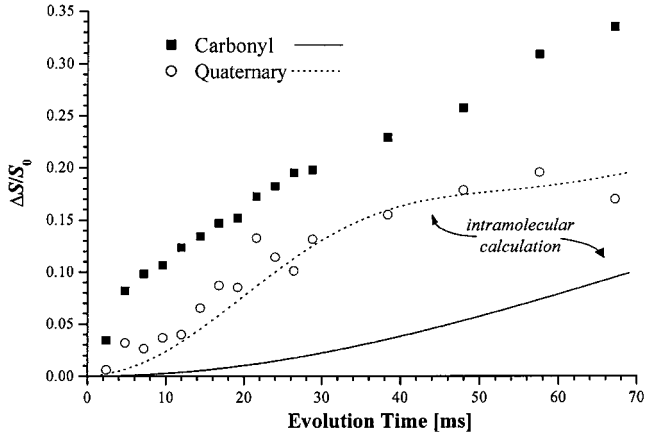

Figure 3. Experimental total (symbols) and calculated intramolecular (solid and dotted lines) $^{13}C\{^2H\}$ REDOR dephasing for carbonyl and quaternary carbons of the linear phenol−polycarbonate of Figure 2. Scatter in the quaternary carbon dephasing is the result of low sensitivity.

data point is about 7% and 24% for the carbonyl and quaternary carbon dephasing, respectively. These standard deviations are based on repeated experiments, some of which had different numbers of ^{13}C refocusing π pulses (see Experimental Methods). In all cases, regardless of the evolution time or number of ^{13}C pulses, the carbonyl carbon dephasing exceeded that of the natural abundance quaternary carbon.

Also shown in Figure 3 is the calculated intramolecular depasing for an all-trans chain conformation. For the carbonyl carbon, the calculation assumed two neighboring phenolic deuterons, each approximately 10 Å away. For the quaternary carbon, three intramolecular $^2H-^{13}C$ dipolar couplings were included. The separation of the phenol ^2H and the carbonyl carbon of the same repeat unit is a 6 Å pseudo two-bond distance that is

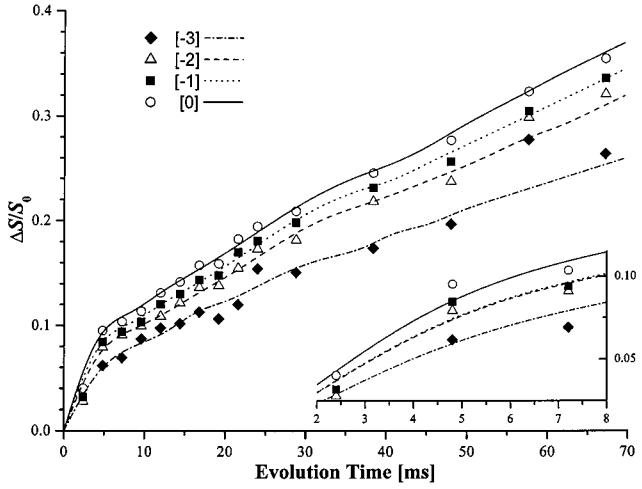

Figure 4. REDOR dephasing ($\Delta S / S_0$) for the centerband and high-field spinning sidebands of the carbonyl carbon resonance of the phenol−polycarbonate of Figure 2 as a function of the dipolar evolution time. The solid and dotted lines connecting the experimental data points are a guide to the eye. A random distribution of orientations of the $^2H-^{13}C{=}O$ internuclear vector relative to the carbonyl carbon chemical shift tensor would result in equal dephasing for the centerband and all sidebands. Calculated dephasing with $\alpha_D = 30°$, $\beta_D = 70°$, and $f = 0.66$ after a short dipolar evolution time is shown in the inset.

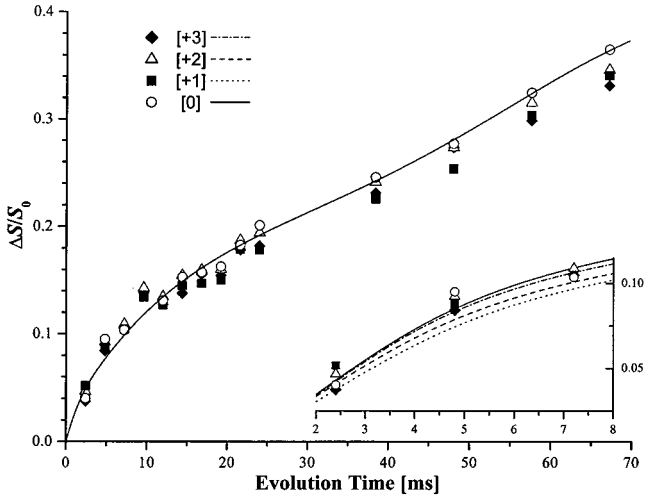

Figure 5. REDOR dephasing ($\Delta S / S_0$) for the centerband and low-field spinning sidebands of the carbonyl carbon resonance of the phenol−polycarbonate of Figure 2 as a function of the dipolar evolution time. The solid line for the centerband is drawn as a reference. Calculated dephasing with $\alpha_D = 30°$, $\beta_D = 70°$, and $f = 0.66$ after a short dipolar evolution time is shown in the inset.

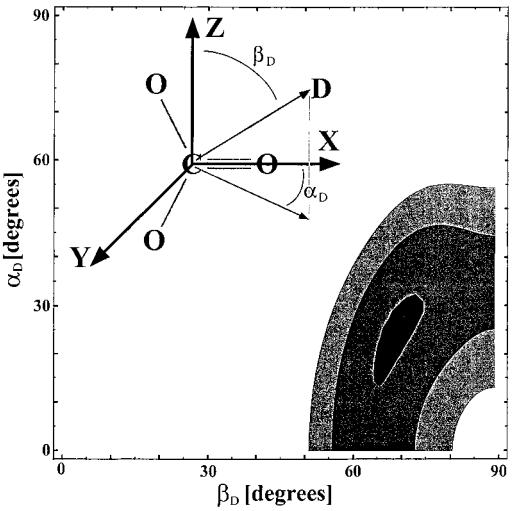

Figure 6. Best-fit contour plot of χ^2 for the orientation of the $^2H-^{13}C{=}O$ vector and the carbonyl carbon chemical shift tensor for those pairs of chains with the largest REDOR dephasing. Each contour represents a 50% increase in χ^2 with the darkest being the lowest value. The inset identifies the α_D (azimuthal) and β_D (polar) orientation of the $^{13}C-^2H$ vector relative to the carbonyl carbon chemical shift tensor. The polycarbonate main-chain axis is essentially along the *Z* axis of the carbonyl carbon chemical shift tensor (see refs 2 and 3). The *X* and *Z* axes and the carbonate group are in the plane of the paper.

independent of conformation. The two next-nearest-neighbor distances were each estimated as 14 Å. These distances were extracted from molecular modeling of chain conformations that will be described later. The calculations assumed 65% deuteration, and the parameters p_1 and p_2 (eq 2) were both set to 0.15. These values for p_1 and p_2 reproduce the long evolution time quaternary carbon dephasing (Figure 3), which suggests an efficiency of about 50% for the ^2H π pulses.[14] This estimate is an upper limit because the intermolecular contributions to the quaternary carbon dephasing were not included. In the calculations, the 6 and 10 Å distances governed the dephasing for the carbonyl and quaternary carbons, respectively. The qualitative features of the dephasing were not significantly affected by reasonable choices of p_1, p_2, percent deuteration, or local conformation. Regardless of the values chosen for these parameters, the calculated intramolecular dephasing for the carbonyl carbon was always less than that for the quaternary carbon.

Figures 4 and 5 show the dephasing of the high- and low-field spinning sidebands of the carbonyl carbon. From Figure 4, it is apparent that the high-field sidebands dephase at significantly different rates and that their ranking (fastest to slowest) is maintained as the evolution time increases. The low-field sidebands, however, dephase at nearly equal rates. To obtain the CSA dipolar orientation from these data, the relative dephasing rates (eq 3) for evolution times of 4.8, 7.2−9.6, 12−14.4, 16.8−19.2, and 21.6−24 ms were compared to calculated values with λ_D's of 0.25, 0.5, 0.75, 1.0, and 1.25, respectively. The bar indicates an average value was used. For these evolution times, the λ_D's correspond to a nearest-neighbor $^2H-^{13}C$ distance of about 4.5 Å (see below), which is derived from the initial dephasing rates. For evolution times up to about 20 ms, the intramolecular dephasing is more than an order of magnitude smaller than the observed rate and can be neglected (Figure 3). If we assume that only a fraction, f, of the $^2H-^{13}C$ dipolar vectors have the same orientation relative to the carbonyl carbon shift tensor, and the remainder, $1 - f$, are randomly oriented (eq 4), then the best fit to the observed dephasing rates for short evolution times is obtained for $f = 0.66$ and an orientation of $\alpha_D = 30°$ (azimuthal) and $\beta_D = 70°$ (polar). A contour plot of $\chi^2[\alpha_D, \beta_D, f = 0.66]$ (eq 5), with the orientation identified in the inset, is shown in Figure 6. The insets in Figures 4 and 5 show the calculated sideband dephasing rates for short evolution times. These calculations assumed 65% deuteration, the above order and orientation parameters, and an exponentially decaying distribution of nearest-neighbor distances that started at 2.5 Å and had an average of 4.5 Å.

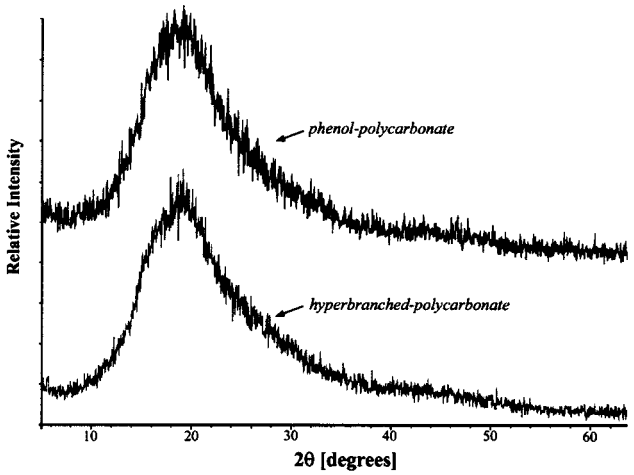

Figure 7. X-ray powder diffraction patterns of the linear phenol−polycarbonate of Figure 2 (top left) and a noncrystalline hyperbranched polycarbonate with the same chemical composition.

Error Analysis for Orientational Parameters for Phenol−Polycarbonate. In the discussion of the previous section, there is some uncertainty as to the λ_D's that correspond to a particular experimental evolution time. This is the situation because the large quadrupolar coupling of the phenolic deuteron means the ^{2}H dephasing pulses are imperfect, and this, in turn, complicates the distance determination that leads to λ_D. The uncertainty is of particular importance in the determination of f because this parameter scales the differences in the sideband dephasing rates. Changing the scaling is similar to shifting the evolution time. This complication was partially overcome by comparing the *relative* dephasing rates for phenol−polycarbonate, which depend on the sideband ranking and not their magnitude. To gauge the error in the fitted values of α_D, β_D, and f, χ^2 was also calculated with λ_D's based on average distances varying from 3.5 to 5.5 Å. This variation represents significant shifts with respect to the λ_D's, and the corresponding experimental evolution times that were used in Figure 6. Nevertheless, in all the calculations, the best-fit orientations were similar, which shows that α_D and β_D are strongly dependent on their sideband ranking. From these calculations, we estimate an uncertainty of ±4° in the values of α_D and β_D and ±10% for f. The parameters p_1 and p_2 might also lead to errors in the fitted parameters. However, perhaps fortuitously, the finite ^{2}H pulses did not affect the determination of α_D, β_D, and f significantly. For example, using the alanine p_1 and p_2 parameters (0.03 and 0.539, respectively) changed the best-fit Euler angles for phenol−polycarbonate to $\alpha_D = 40°$ and $\beta_D = 62°$, variations of only 10° from the values of Figure 6. No qualitative conclusions based on the orientation parameters are affected by this sort of uncertainty.

Powder Diffraction. The orientational preferences in chain packing detected by REDOR must be short-range (restricted to just a few neighboring chains) because there is no evidence of long-range order or crystallinity by X-ray powder diffraction (Figure 7). The diffraction patterns for phenol−polycarbonate and a noncrystalline hyperbranched polycarbonate[12] of identical composition are indistinguishable from one another and from published diffraction patterns for amorphous polycarbonate[19] and polystyrene.[19] The scattering maximum near $2\Theta = 20°$ results from general interatomic spacings and is not evidence for order associated with specific distances or orientations.[19]

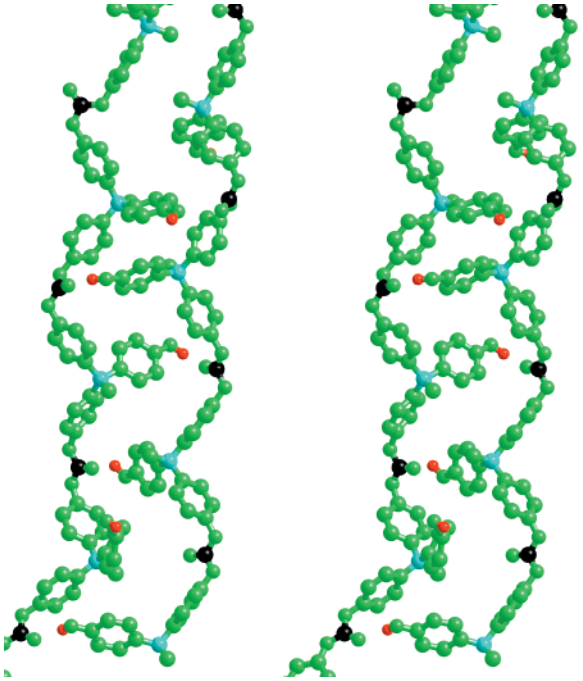

Figure 8. Stereoview of two linear phenol−polycarbonate chains showing the proximity of the phenol ring of one chain (^{2}H in red) and the carbonate of another chain (^{13}C in black) in the Whitney−Yaris packing of nearest-neighbor chains. The quaternary carbons are shown in light blue.

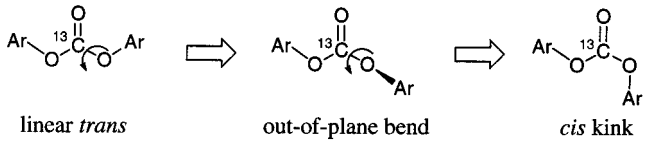

Figure 9. Local conformational rearrangements of the carbonate linkage of linear polycarbonates.

Molecular Modeling. A stereoview of the Whitney−Yaris spatial arrangement for nearest-neighbor chains is shown in Figure 8. Combining this arrangement for pairs of chains with a mixture of chain-pair directions, and the sorts of twists and bends (Figure 9) found in the random-packing model, produces a chain-pair packing model for phenol−polycarbonate that has no hint of long-range order (Figure 10, bottom left). Although similar in their long-range attributes, the random and chain-pair packing models differ in their distributions of nearest-neighbor distances and local orientations. For the random-packing model, the nearest-neighbor distance distribution is similar to a Gaussian centered around 5 Å with a half-height full width of about 3 Å. This distribution produces too little initial dephasing to match the data. The corresponding distribution for the chain-pair packing model is biased toward short distances and reproduces the observed initial dephasing well. In fact, the exponential distribution used in the calculated dephasing shown in the insets to Figures 4 and 5 mimics the distribution of the chain-pair packing model.

The differences in local orientation for each model are apparent from their calculated sideband dephasing, which can be calculated accurately (eqs 1 and 2) because the locations of all the deuterons close to each carbonyl carbon are known. For the random-packing model, all the sidebands, including the low-field sidebands (not

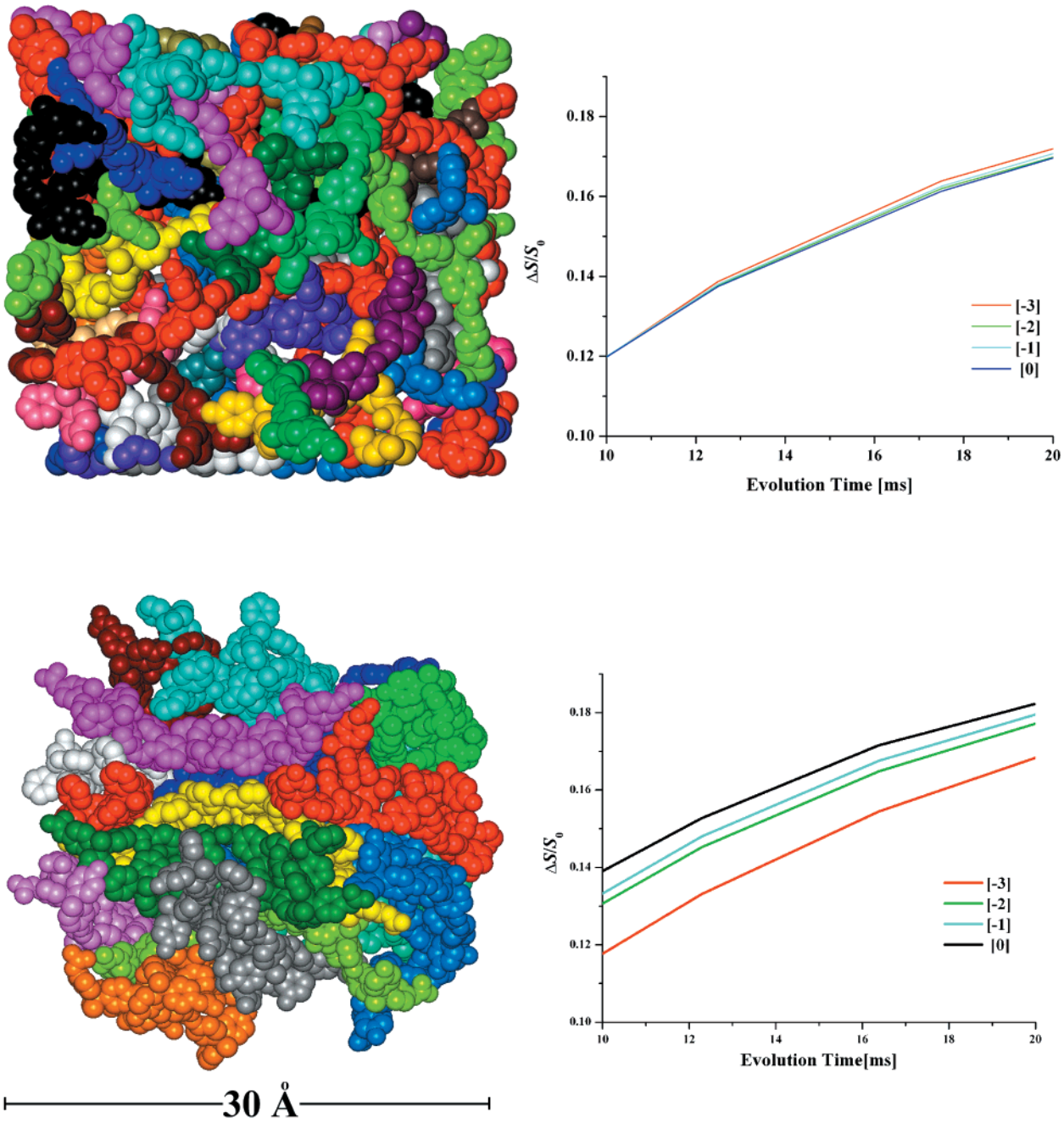

Figure 10. Molecular models and associated calculated REDOR sideband dephasing ($\Delta S / S_0$). The calculations included multispin dipolar couplings and corrections for imperfect ^{2}H pulses. (top left) random-packing model; (top right) calculated high-field sideband dephasing for the random-packing model model; (bottom left) chain-pair packing model; (bottom right) calculated high-field sideband dephasing for the chain-pair model.

shown), dephase at essentially the same rate (Figure 10, top right), which is consistent with an isotropic distribution of carbonyl deuteron orientations. The minor differences present for longer evolution times result from variations in intramolecular dephasing. In contrast, the sidebands for the chain-pair model dephase at significantly different rates (Figure 10, bottom right), indicative of preferred orientations for the carbonyl carbon of one chain and the deuteron of another.

Specification of the locations in the chain-pair packing model of the three nearest deuterons for each carbonate group permitted a confirmation of the assertion that the *initial* carbonyl carbon dephasing rates are dominated by the nearest-neighbor deuteron. Calculations of the REDOR dephasing assuming dipolar $^{13}C-^2H$ coupling to only the nearest-neighbor deuteron, and to the three nearest deuterons, were within 10% of one another for total dephasing (sum of centerband and all sidebands) after 8 ms of dipolar evolution. The rankings for sideband dephasing rates were identical for the two calculations.

The $^{13}C-^2H$ pair-distribution functions for the carbonyl and quaternary carbons of the random-packing model (Figure 11) are similar to those presented by Hutnik et al.[1] The corresponding functions for the chain-packing model are shown in Figure 12. The pair distribution function, $g(r)$, can be thought of as the number of atoms a distance r from a given atom, compared with the number at the same distance in an ideal gas at the same density.[20] For small r, less than typical van der Waals radii, $g(r)$ is zero, and for large r, $g(r)$ approaches unity if there is no long-range order.

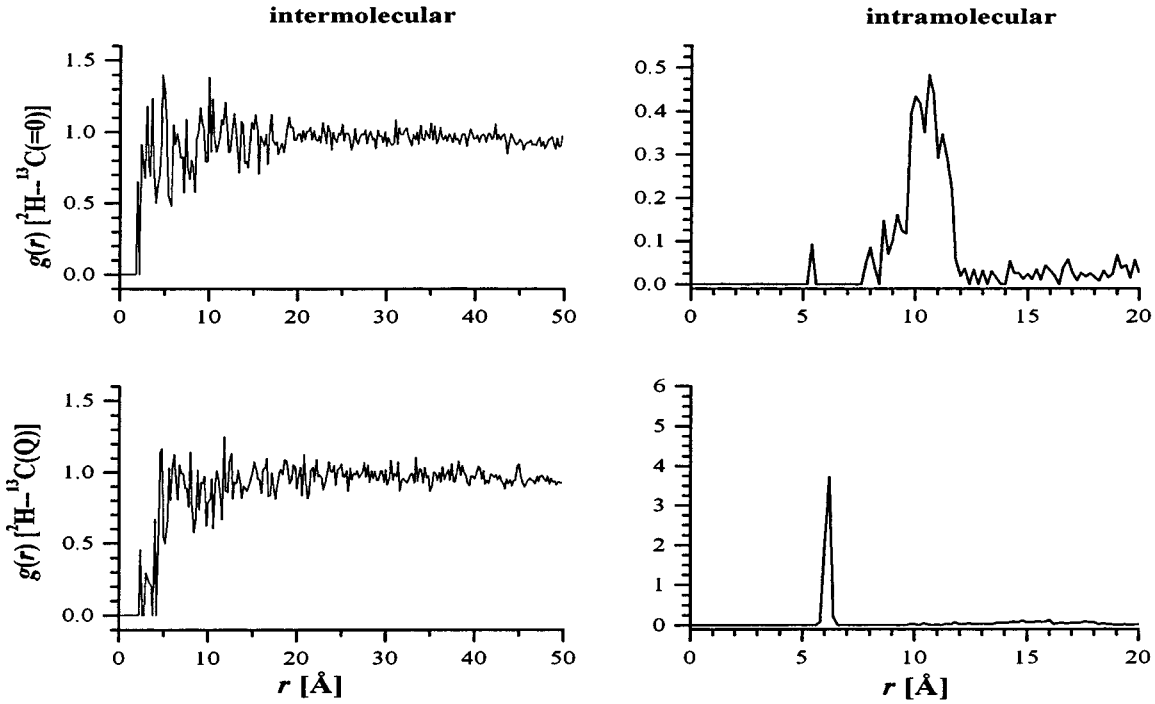

Figure 11. Calculated distance pair distribution functions for a random-packing model of linear phenol−polycarbonate. The interchain distribution functions (left, top and bottom panels) are similar to those reported by Hutnik et al. (ref 1) for bisphenol A polycarbonate. The intrachain $^{2}H\cdots$quaternary carbon separation of 6 Å (lower right panel) is a pseudo-two-bond distance.

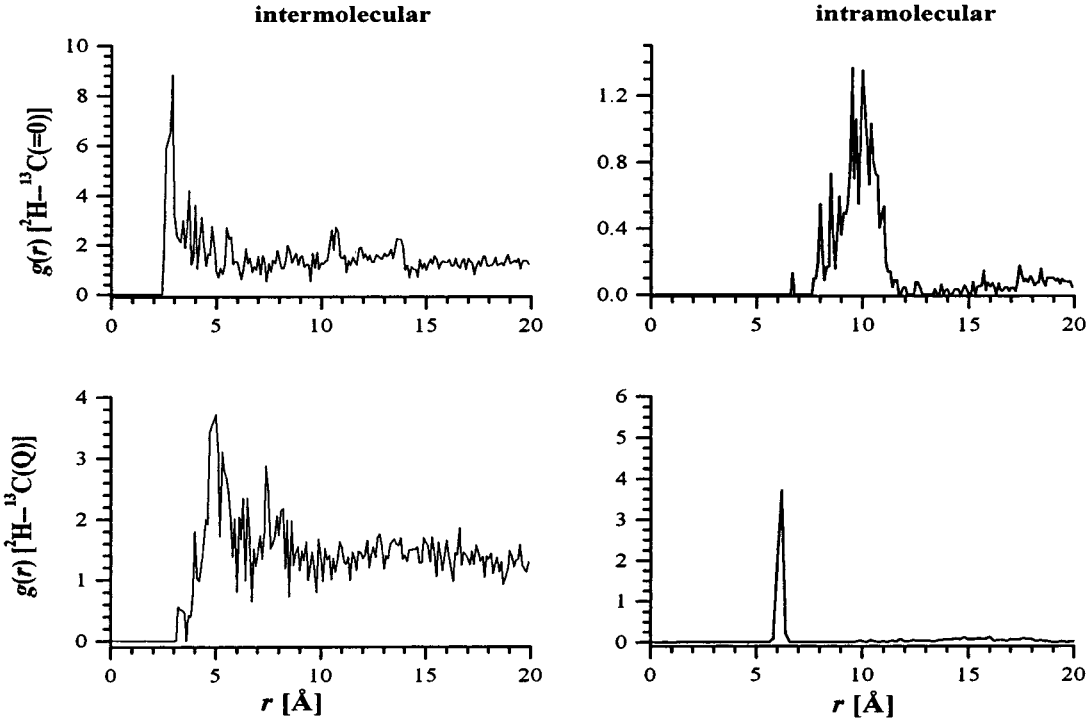

Figure 12. Calculated distance pair distribution functions for the chain-pair packing model of linear phenol−polycarbonate shown in Figure 10 (lower left). The matrix of 24 pairs of chains had 120 interchain distances of less than 5 Å between the phenol ^{2}H of one chain and the carbonate ^{13}C of the nearest-neighbor chain. The intrachain pair functions (right column) are essentially the same as those calculated for the random-packing model in Figure 11.

The limited chain lengths of the models preclude the intrachain $g(r)$s from reaching unity. Both models have intrachain $g(r)$s that show the expected intra-repeat-unit preferences and interchain $g(r)$s asymptotes that are consistent with the absence of long-range order. In particular, the 6 and 10 Å $^{2}H-^{13}C$ intramolecular nearest-neighbor distances for the quaternary and carbonyl carbons, respectively, are clearly identified. These are the most important distances used in the dephasing calculation of Figure 3. Differences between the two models appear in the interchain pair-distribution functions at small r. For the random-packing model, the carbonyl and quaternary carbon $g(r)$s are about the same and show no distance preferences, which confirms the isotropic nature of the model. By contrast, for the chain-pair model, the carbonyl and quaternary carbon

interchain $g(r)$s are significantly different and show the preference for shorter carbonyl carbon to deuteron distances that was built into the model.

The calculated total dephasing for the two models (not shown) paralleled the trends for these $g(r)$s. For the random model, the dephasing due to intermolecular dipolar interactions was equal for the carbonyl and quaternary carbons, whereas the dephasing due to the intramolecular dipolar interactions was not. This resulted in the total dephasing calculated for the quaternary carbon *always* exceeding that for the carbonyl carbon. For the chain-pair model, the intermolecular $^{13}C-^{2}H$ distances are not comparable, and the calculated dephasing for the carbonyl carbon exceeded that for the quaternary carbon for evolution times less than 20 ms. After 20 ms, most of the proximate, nonrandom intermolecular $^{13}C-^{2}H$ pairs had completely dephased. The calculated dephasing for both random and chain-pair models was similar for longer evolution times, in disagreement with experiment (Figure 3). Preliminary calculations have shown that adding more close intermolecular carbonyl−phenol contacts, possibly arising from multichain alignments, improved the agreement.

Discussion

REDOR Sideband Analysis. The attractive features of $^{13}C\{^{2}H\}$ REDOR as a general method for determination of specific orientation in polymers are that it is (i) one-dimensional and hence high sensitivity, (ii) chemical-shift specific because of magic-angle spinning, (iii) accessible to any site that can be labeled by ^{2}H, (iv) adaptable to clusters of two or more ^{2}H labels, and (v) suitable for simple spin counting for quantitative analysis. For systems in which a few ^{19}F labels can be introduced without significant structural perturbations, $^{13}C\{^{19}F\}$ REDOR offers the additional possibility of detection of local order in polymer glasses measured on a 20 Å scale, twice that of the $^{13}C\{^{2}H\}$ REDOR experiments reported here.

Local Order in Phenol−Polycarbonate from REDOR. A comparison of the total dephasing of the carbonyl and quaternary carbon resonances indicates that phenol−polycarbonate is an ordered system. If phenol−polycarbonate were randomly packed, all intermolecular interatomic spacing distributions would be equivalent (see Figure 11, left, top and bottom). This would mean that the intermolecular dephasing would be equal for all carbons, and the intramolecular proximity of ^{13}C and ^{2}H labels would ensure that the dephasing for the quaternary carbon always exceeded that for the carbonyl carbon. Exactly the opposite is observed. Thus, to be consistent with both the REDOR and X-ray results, the chains must be packed with some degree of local order but no long-range order.

Although interpreting the total dephasing for long evolution times quantitatively in terms of a distribution of $^{13}C-^{2}H$ distances is complicated by the finite ^{2}H pulses, a comparison of the *initial* dephasing for the quaternary and carbonyl carbons, which is dominated by the single, nearest-neighbor deuteron, indicates that the average interchain spacing between a carbonyl carbon and its nearest-neighbor deuteron is 4.5 Å. This comparison is based on the intramolecular quaternary carbon−deuteron distance of 6 Å, with any intermolecular quaternary carbon−deuterons less than 6 Å excluded. Thus, the 4.5 Å $^{2}H-^{13}C$ distance for the carbonyl carbon is an upper limit.

Orientation information in REDOR is contained in the relative dephasing rates of the spinning sidebands.[21] The first step in obtaining this information is to infer a distribution of nearest-neighbor distances from the total REDOR dephasing. Then, the appropriately weighted sideband dephasing is calculated for each experimental (short) evolution time, so that the determination of α_D, β_D, and f is model-independent. This is a general strategy for using REDOR to obtain orientational information, which is analogous to the use of the familiar Herzfeld−Berger maps[22] to characterize chemical shift tensors from sideband intensities. Full spectral simulations are not required.

For phenol−polycarbonate, the $^{13}C\{^{2}H\}$ dephasing of the carbonyl carbon spinning sidebands depends on the relative orientation of the interchain $^{13}C-^{2}H$ internuclear vector with respect to the carbonyl carbon chemical shift tensor. In an isotropic arrangement of orientations, the sidebands and centerband dephase at the same rate.[9,21] The high-field spinning sidebands of the carbonyl carbon of the $^{13}C-^{2}H$-labeled phenol−polycarbonate dephase at significantly different rates from each other (Figure 4), whereas the low-field sidebands dephase at about the same rate (Figure 5). Observation of these differences in dephasing rates proves that the chains are packed with preferred orientations, consistent with the local-order conclusion based on total dephasing. The best calculated fit to the observed dephasing rates for short evolution times (Figures 4 and 5, inset) is obtained for 66% of all chains with angles $\alpha_D = 30°$ (azimuthal) and $\beta_D = 70°$ (polar) describing the orientation of the $^{2}H-^{13}C$ dipolar vector relative to the carbonyl carbon shift tensor. These determinations are independent of any model for chain packing.

With the polycarbonate main-chain axis essentially along the Z axis of the carbonyl carbon chemical shift tensor,[2,3] and the carbonyl carbon−oxygen double bond defining the X-axis direction,[2,3] the $^{13}C-^{2}H$ distance and orientation suggest that hydrogen bonds might form between the phenols of one chain and the carbonates of another (see Figure 6, inset, and Figure 8). Hydrogen bonds could account for the observed broad ^{2}H powder pattern and the high (210 °C) T_g of phenol−polycarbonate. However, REDOR results similar to those of Figures 3−5 have also been obtained for an ethoxyphenyl-substituted bisphenol A polycarbonate, a system for which there is no possibility of hydrogen-bond formation.[9] Thus, even though hydrogen bonds might be present in phenol−polycarbonate, hydrogen-bond energetics are not the likely driving force for the formation of local order.

Chain-Pair Packing Model for Phenol−Polycarbonate. The Whitney−Yaris pairwise packing of chains illustrated in Figure 8 is a reasonable way to accommodate both the distance and orientation restraints of Figures 3−6 in phenol−polycarbonate. The first depictions of this model applied to bisphenol A polycarbonate showed locally parallel chain segments as linear two-dimensional arrays[5] or as simple cylinders in three-dimensional cartoon form.[4] These linear arrays were useful for involved dynamics calculations, and the cylinders were certainly easy to draw, but both gave an unintended impression of long-range order despite the written disclaimers. Adding turns and bends to variations in spacings for *pairs* of chains in the packed glass avoids the possibility of any long-range order while still

preserving the inherent physics of the Whitney−Yaris pair. This was the motivation for building the chain-pair model of Figure 10 (bottom left). The local order of this model is confirmed by the calculated sideband dephasing (Figure 10, bottom right) and calculated $g(r)$s (Figure 12). A more elaborate model might have individual chains swapping partners and occasionally aligning with more than just a single nearest neighbor. Thus, the present chain-pair model should be thought of as the most rudimentary model[23] that can account for the local order demanded by the REDOR dephasing and still be consistent with the absence of crystalline long-range order.

Local Order in Bisphenol A Polycarbonates. The tight packing of locally parallel trans chain segments described above for phenyl-substituted polycarbonates has also been inferred from the results of relaxation[24] and homonuclear[4] and heteronuclear[24,25] recoupling experiments for bisphenol A polycarbonate as well as for a variety of other linear polycarbonate homopolymers and copolymers.[23] Although none of these experiments constitutes a direct measure of local order, the sum total of all of the evidence seems compelling. The molecular basis for such a packing preference in polycarbonates may be that the lock-and-key fit of the phenol (or ethoxyphenyl or isopropylidene) of one chain and the carbonate of another results in an interdigitation of chains which entropically[26] biases the population of conformations and creates local order in the condensed phase.[27] By this view, the formation of the glass, either quickly by precipitation in a nonsolvent or slowly under pressure in a melt press, is driven by the minimization of repulsions.[28] Naturally, long-range attractive van der Waals and hydrogen-bond interactions are present, influence the assemby of chains in solution or in the melt,[29] and play a role in determining the final distribution of packing conformations in the glass. But they are of secondary importance in determining the sort of local order indicated in Figure 6.

The chain-pair packing model is fully consistent with the extent of distance and orientational order reported earlier for unsubstituted bisphenol A polycarbonates.[2,4] As long as the order in polycarbonates is truly local, then ordered regions will contain only a few chains (sometimes referred to as bundles)[4,5] and the length of these regions can extend only a few repeat units. Even for a four-chain bundle, for example, all the chains have near neighbors that are part of other bundles with differing mainchain directions[4] or that are part of the disorganized matrix. The model structures analyzed and dismissed by Schmidt-Rohr et al.[30] are crystals, not bundles, because all carbonyl carbon shift tensors in these structures have the identical orientation relative to one another. Interbundle proximities are especially important for the carbonate groups which are not close to one another in a Whitney−Yaris pair (Figure 8). Thus, the results of the carbonate−carbonate $^{13}C-^{13}C$ polarization transfer experiments of Robyr et al.,[2] in which preferences for bisphenol A polycarbonate mainchain directions perpendicular as well as parallel to one another were detected, are not evidence against bundle formation. Rather, the observations by Robyr et al.[2] are fully interpretable within the context of the bundle model and, moreover, suggest that there are preferences in interbundle orientations.

Acknowledgment. This work was supported by U.S. Army Research Office Grant DAAG5-97-1-0183 (K.L.W.) and NSF Grant DMR-97202 (J.S.). A Pfizer Undergraduate Summer Research Fellowship and a Waldo Semon Undergraduate Research Grant sponsored by B. F. Goodrich (J.A.B.) are also gratefully acknowledged. The authors thank Professor Frank Blum (University of Missouri, Rolla) for the generous access to his ^2H NMR spectrometer. The authors also thank Tomasz Kowalewski (Carnegie Mellon University, Pittsburgh) for acquisition of the X-ray powder diffraction data of Figure 7.

References and Notes

(1) Hutnik, M.; Argon, A. S.; Suter, U. W. *Macromolecules* **1991**, *24*, 5970.
(2) Robyr, P.; Gan, Z.; Suter, U. W. *Macromolecules* **1998**, *31*, 6199.
(3) Utz, M.; Atallah, A. S.; Robyr, P.; Widmann, A. H.; Ernst, R. R.; Suter, U. W. *Macromolecules* **1999**, *32*, 6191.
(4) Klug, C. A.; Zhu, W.; Tasaki, K.; Schaefer, J. *Macromolecules* **1997**, *30*, 1734.
(5) Whitney, D. R.; Yaris, R. *Macromolecules* **1997**, *30*, 1741.
(6) Červinka, L.; Fischer, E. W.; Hahn, K.; Jiang, B.-Z.; Hellman, G. P.; Kuhn, K.-J. *Polymer* **1987**, *28*, 1287.
(7) Červinka, L.; Fischer, E. W.; Dettenmaier, M. *Polymer* **1991**, *32*, 12.
(8) Gullion, T.; Schaefer, J. *Adv. Magn. Reson.* **1989**, *13*, 57.
(9) O'Connor, R. D.; Byers, J. A.; Arnold, W. D.; Oldfied, E.; Wooley, K. L.; Schaefer, J. *Macromolecules* **2002**, *35*, 2618.
(10) Gullion, T.; Baker, D.; Conradi, M. S. *J. Magn. Reson.* **1990**, *89*, 479.
(11) O'Connor, R. D.; Blum, F. D.; Ginsburg, E.; Miller, R. D. *Macromolecules* **1998** *31*, 4852.
(12) Bolton, D. H.; Wooley, K. L. *Macromolecules* **1997**, *30*, 1890.
(13) O'Connor, R. D.; Schaefer, J. *J. Magn. Reson.* **2002**, *154*, 46.
(14) Sack, I.; Vega, S. *J. Magn. Reson.* **2000** *145*, 52.
(15) Butler, L. G.; Brown, T. L. *J. Am. Chem. Soc.* **1981**, *103*, 6541.
(16) Schmidt-Rohr, K.; Spiess, H. W. *Multidimensional Solid State NMR and Polymers*; Academic Press: London, 1994; p 236.
(17) Schaefer, J.; Stejskal, E. O.; Buchdahl, R. *Macromolecules* **1977**, *10*, 384.
(18) Stothers, J. B. *Carbon-13 NMR Spectroscopy*; Academic Press: New York, 1972; p 494.
(19) Fitzpatrick, J. R.; Ellis, B. X-ray Diffraction Studies of the Structure of Amorphous Polymers. In *The Physics of Glassy Polymers;* Haward, R. N., Ed.; John Wiley & Sons: New York, 1973; pp 120−125.
(20) Hirschfelder, J. O.; Curtiss, C. F.; Bird, R. B. *Molecular Theory of Gases and Liquids*, John Wiley & Sons: New York, 1966; p 320.
(21) Goetz, J. M.; Schaefer, J. *J. Magn. Reson.* **1997**, *127*, 222.
(22) Herzfeld, J.; Berger, A. E. *J. Chem. Phys.* **1980**, *73*, 6021.
(23) Goetz, J. M.; Wu, J.; Yee, A. F.; Schaefer, J. *Macromolecules* **1998**, *31*, 3016.
(24) Lee, P. L.; Kowalewski, T.; Poliks, M. D.; Schaefer, J. *Macromolecules* **1995** *28*, 2476.
(25) Schmidt, A.; Kowalewski, T.; Schaefer, J. *Macromolecules* **1993**, *26*, 1729.
(26) Frenkel, D. *Phys. World* **1993** *6*, 24.
(27) Davidchack, R. L.; Laird, B. B. *J. Chem. Phys.* **1998** *108*, 9452.
(28) Davidchack, R. L.; Laird, B. B. *Phys. Rev. Lett.* **2000** *85*, 4751.
(29) Weeks, J. D.; Selinger, R. L. B.; Broughton, J. Q. *Phys. Rev. Lett.* **1995**, *75*, 2694.
(30) Schmidt-Rohr, K.; Bonagamba, T. J.; deAzevedo, E. R.; Dunbar, M. G.; Becker-Guedes, F.; Harris, D. J.; Kaji, I. I. Presented at the San Francisco ACS Meeting, March 2000.

MA010919I